

## EXPERIMENTAL STUDY ON HIDDEN CORROSION/DELAMINATION DETECTION WITH ULTRASONIC GUIDED WAVES

Wenhao Zhu, Joseph L. Rose  
Dept of Engineering Science and Mechanics  
The Pennsylvania State University  
University Park, PA 16802

Vinod S. Agarwala  
Naval Air Warfare Center  
Patuxent River, MD 20670

### INTRODUCTION

Hidden corrosion detection is critical in the aerospace industry. Occurring on the inside surfaces or at the interfaces of an aircraft's skin, the corrosion must be detected from the outside surface. Surface waves are, therefore, not suitable for detecting such defects/failures. Ultrasonic bulk wave methods can be used to detect the corrosion caused thinning in the wall or a delamination of a structure [1,2]. However, since the method is based on point-by-point testing, it becomes a tedious time consuming procedure for large area inspection. Guided wave methods are being developed to tackle this problem [3-6]. An experimental study of hidden corrosion/delamination detection in single/multiple layer aluminum plates is conducted with specially selected ultrasonic guided wave modes. Both corrosion simulation specimens by machine cutting, and real corrosion specimens by electrochemical processing, are used in the investigation with a wide range of corrosion depths from 0.03mm to 0.6mm. Two-layer specimens have been prepared with such corroded sheets to form an artificial interface corrosion/delamination. Various wave modes are subsequently generated on these specimens to examine the implications of thinning on mode cutoff, group velocity changes, mode frequency shifts, and transmission and reflection amplitudes. Finally, a practical problem of skin to honeycomb core delamination detection with guided waves is also addressed.

### SPECIMENS AND EXPERIMENTAL METHODOLOGY

Three types of aluminum corrosion specimens were prepared and used in the guided wave experimental work: (1) single layer plates with simulation corrosion prepared by machine cutting as shown in Fig1. The corroded zone surfaces are smooth and the depths are made at 5%, 10%, and 20% of the 1.62mm plate thickness, respectively. (2) single layer real corrosion plates prepared by a controlled electrochemical procedure as shown in Fig.2. Artificial seawater (ASTM Standard D112) was applied and the specimens were subjected to

static overpotentials for 12-24 hours at a current density of  $1.4\mu\text{A}/\text{cm}^2$ . The average corrosion depths were from 0.03mm to 0.6mm for different specimens. Non-uniform corrosion depths were also made on the same aluminum sheet, the depth changing from 0.03mm to 0.27mm along the section. Generally, the corroded zones have rough surfaces. (3) two-layer interface corrosion specimens prepared synthetically by adhering two plates together with sealant, one sheet having a real or simulated corrosion zone as shown in Fig.3. Both corrosion simulation and real corrosion sheets are used to fabricate the two-layer specimens. The experimental setup for the ultrasonic guided wave is shown in Fig.4. Oblique incidence and receiving are applied in a through-transmission scheme with the wedge angle being adjustable. Because guided wave modes depend on the frequency-thickness product and interface quality, there is a possibility of detecting corrosion thinning as well as interface corrosion/delamination of the structure with guided waves. In particular, at least four methods can be considered in the testing: (1) the wave mode cutoff approach, (2) the time of flight and group velocity change, (3) the mode frequency shifts, especially for interface corrosion, and (4) the relative transmission and reflection amplitudes. All of these methods offer the potential of inspecting hidden surface and interface corrosions in such structures as aircraft skins. For different problems, there are different advantages and disadvantages of the guided wave approaches compared to the bulk wave techniques. It is therefore wise to compare the different methods and to select the best features for a specific problem.

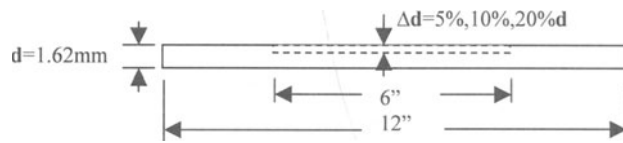


Fig.1 Corrosion simulation specimens with the depths being 5%,10%,20% of the thickness.

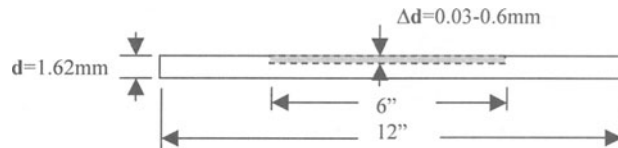


Fig.2 Real corrosion specimens with the depths varying from 0.03 to 0.6mm.

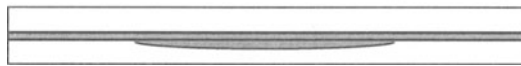


Fig.3 Interface corrosion/delamination specimens.

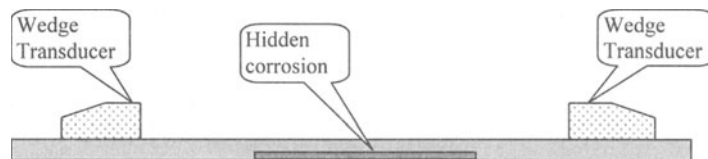
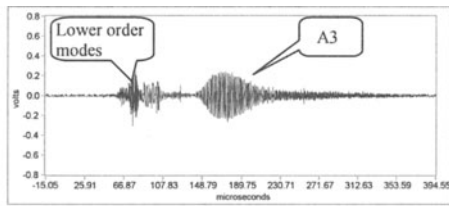
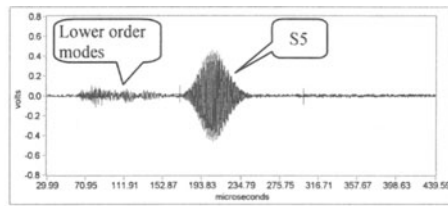


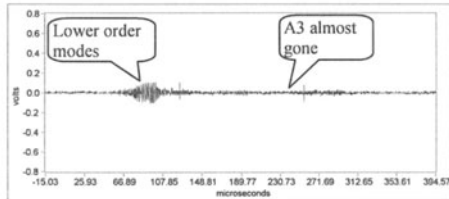
Fig.4 Experimental setup: oblique incidence and reception with wedges.



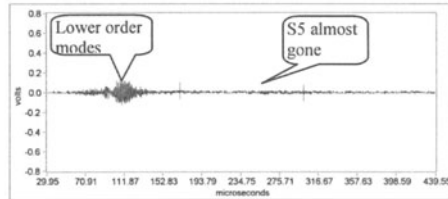
(a) Transmitted A3 RF without corrosion



(c) Transmitted S5 RF without corrosion

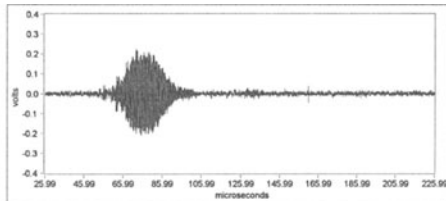


(b) Transmitted A3 RF with 5% corrosion

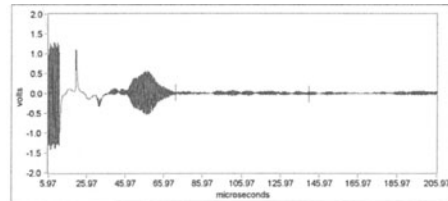


(d) Transmitted S5 RF with 5% corrosion

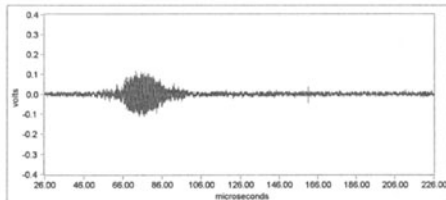
Fig.5 Transmission RF of A3 (a,b) and S5 (c,d) modes at  $25^\circ$  incidence and 4.39 and 6.37 MHz, respectively, for the 1.62mm plates with and without the 5% corrosion zone.



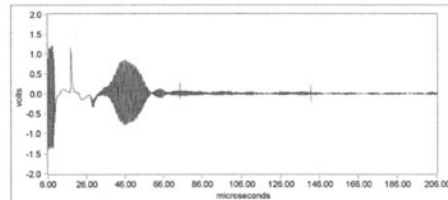
(a) Transmitted modes for the shallow corrosion zone (0.03mm).



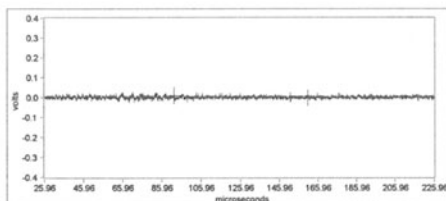
(b) Reflected modes for the shallow corrosion zone (0.03mm).



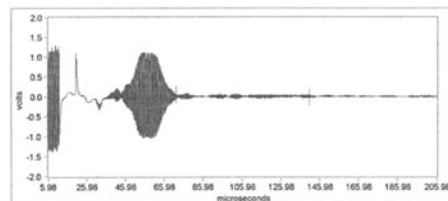
(c) Transmitted modes for the medium corrosion zone (0.15mm).



(d) Reflected modes for the medium corrosion zone (0.15mm).



(c) Transmitted modes for the deep corrosion zone (0.27mm).



(d) Reflected modes for the deep corrosion zone (0.27mm).

Fig.6 Transmission and reflection of wave modes from real corrosions of different depths with a 2.23MHz toneburst and  $15^\circ$  degree incidence.

Table 1. Group velocity changes for the S0 dominant mode packet

Specimens	Frequency	Angle	$C_g$	Relative change
No corrosion	1.75MHz	70°	2.24mm/us	0%
5%	1.75MHz	70°	2.74mm/us	22.3%
10%	1.75MHz	70°	3.16mm/us	41.1%
20%	1.75MHz	70°	3.79mm/us	69.1%

## RESULTS FOR THE SINGLE LAYER HIDDEN CORROSION SPECIMENS

Experiments for hidden surface corrosion detection were carried out on both the simulation and real corrosion specimens. In the phase velocity dispersion curves, each higher order mode (above S0 and A0) has a vertical asymptotical line. When  $f_d$  values are located to the right of the asymptotical line, this mode can exist or can be excited, otherwise the mode will disappear or cutoff. We therefore used a toneburst system to generate modes around the cutoff frequencies. Figure 5 shows the transmission RF signals for the 1.62mm plate with 5% corrosion. The A3 and S5 modes are generated by using 4.39 and 6.37MHz tonebursts which demonstrate the mode cutoff phenomena when passing through the 5% corrosion zone.

Similar results were also obtained for the 10% and 20% corrosion simulation specimens. The same procedure was applied to the non-uniform real corrosion specimens where both the transmitted and reflected waves are recorded. Fig.6 show the transmission and reflection RF signals when interacting with different corrosion depths. As predicted, the deeper the corrosion depth, the higher the reflected amplitude and the lower the transmitted amplitude.

From the received through-transmission RF signals, one can also tell the differences on the time of flight between the signals with and without the corrosion zone. This is related to a group velocity change. Typical results are shown in Table 1. This is also predicted from the group velocity dispersive nature.

## RESULTS FOR THE TWO-LAYER INTERFACE CORROSION SPECIMENS

Experiments for interface corrosion/delamination detection were carried out on both the simulation and real corrosion specimens.

### Guided Wave Modes Cutoff

The guided wave modes cutoff phenomena was also observed when the waves passed through the corroded zones of the two-layer specimens. Fig.7 (a) and (b) shows the received through transmission signals across the no-corrosion and corroded zones, respectively, for an interface corrosion specimen with a 20% corrosion simulation occurring on the top layer. Fig.8 (a) and (b) shows the transmission signals across the good bond and disbond zones respectively in a delaminated two-layer specimen.

Two real corrosion two-layer specimens were also tested with the corrosion depths being 15-30% and 30-45% of the plate thickness, respectively. Fig.9 shows the results for the 30-45% interface corrosion specimen. As seen, there are two modes propagating in the two-layer specimen under this condition, one (first mode) was cut-off by the corrosion zone (occurring on the bottom layer), whereas the other (second mode) still passed through the zone. More interesting, if the interface corrosion occurs on the top layer (the testing side), both modes were cut-off by the corrosion zone. Similar results have also been obtained for the 15-30% interface corrosion specimen. This feature can be used to identify the layer on which the corrosion occurred.

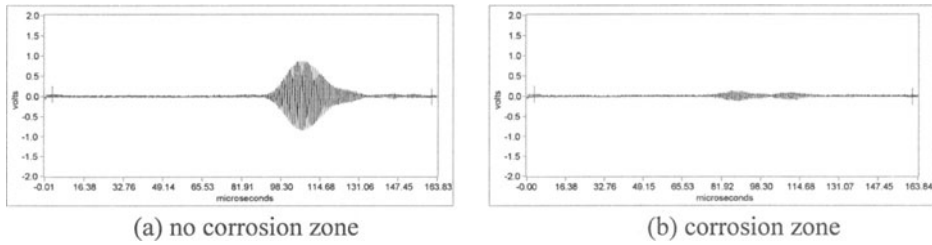


Fig.7 RF signals for the 20% interface corrosion simulation two-layer specimen with a 1.22MHz toneburst at a 10° angle of incidence.

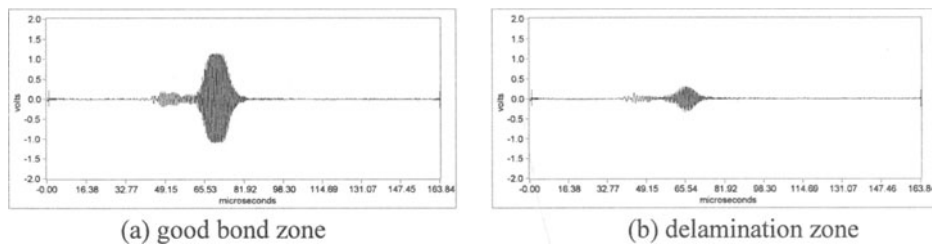


Fig.8 RF signals for the delaminated two-layer specimen with a 4.16MHz toneburst at a 30° angle of incidence.

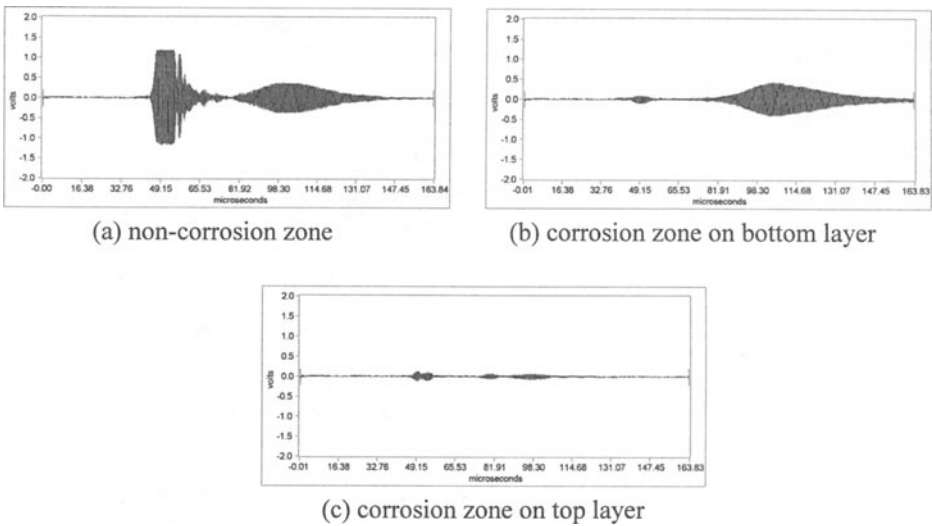
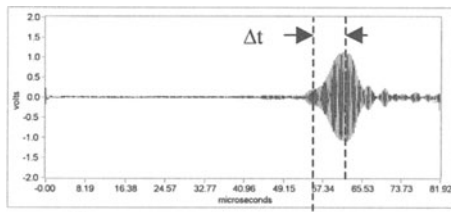
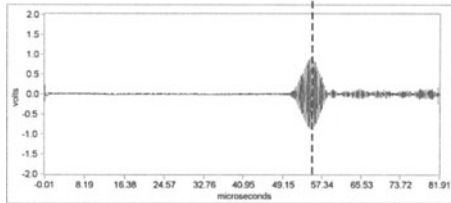


Fig.9 RF signals the 30-45% interface corrosion two-layer specimen with a 3.32MHz toneburst at a 35° angle of incidence.

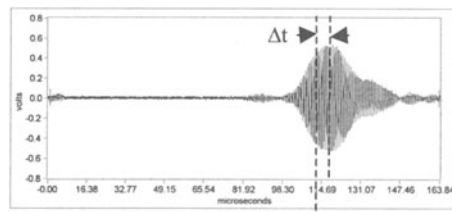


(a) non-corrosion zone

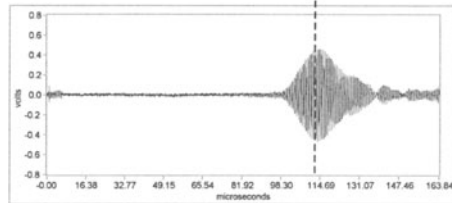


(b) corrosion zone

Fig.10 Time of flight change due to interface corrosion for the 5% corrosion specimen with a 1.22MHz toneburst at a 10° angle of incidence.



(a) non-corrosion zone

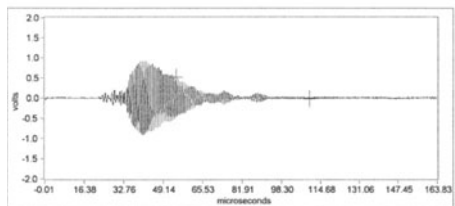


(b) corrosion zone

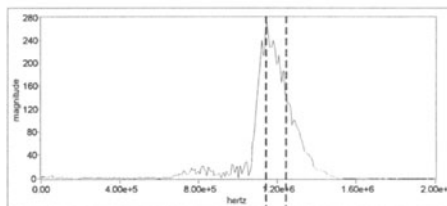
Fig.11 Time of flight change due to interface corrosion for the 10% corrosion specimen with a 3.1MHz toneburst at a 35° angle of incidence.

### Guided Wave Mode Group Velocity Change

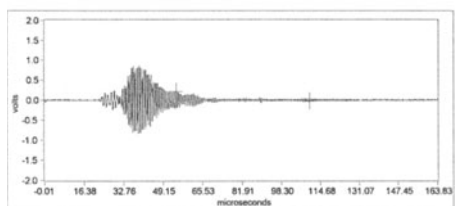
Not all interface corrosion leads to guided wave mode's cut-off. Generally, shallow corruptions can only damp the wave modes instead of destroying them. However, in certain conditions it may take different times for some specific mode to pass through the corrosion and non-corrosion zones of the same length. This corresponds to the mode group velocity changes. Fig.10 and 11 shows the different time of flights of the wave modes for the 5% and 10% corrosion simulation two-layer specimens respectively. Both cases show an increase in the group velocity. However, as mentioned for single layer experiments, the mode group velocity can increase or decrease.



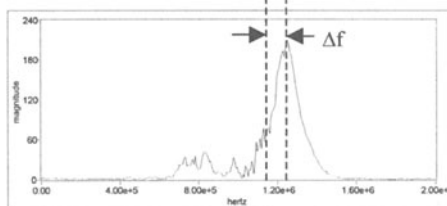
(a) RF signal without the delamination



(b) The FFT of (a)

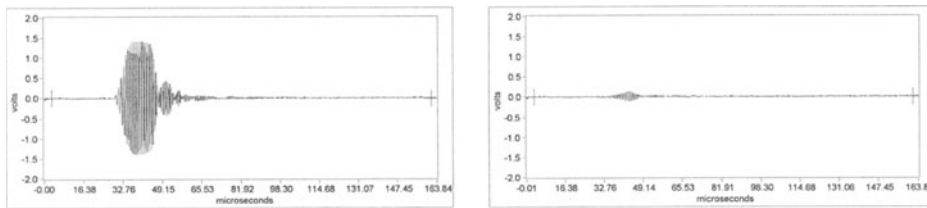


(c) RF signal with the delamination



(d) The FFT of (c)

Fig.12 The transmission RF signals in the two-layer specimen and their corresponding spectrums, with a 1.2MHz toneburst at a 30° angle of incidence



(a) disbond between the skin and core      (b) good bond between the skin and core  
 Fig.13 Recorded Rf signals across a honeycomb specimen with a 1.3MHz toneburst at a 45° angle of incidence.

### Guided Wave Mode Frequency Shift

In certain conditions, guided mode frequency shifts can also be observed for interface corrosion/delamination specimens. Fig.12 shows the mode frequency shift in the received RF for a delaminated two-layer specimen. The time domain signals look similar, except for amplitude damping in the signal through the delamination zone. In the frequency domain, the peak frequency for the wave mode through the delamination zone shifts right corresponding to that without through the delamination zone.

### Honeycomb Specimen

Generally, well bonded honeycomb cores can cause attenuation of the guided waves that are propagating in the skin as a result of leakage at the bonded zone. Guided wave experiments on good bond and poor bond areas of honeycomb specimens demonstrates such a principle. Fig.13 (a) and (b) shows the through-transmission RF signals along the disbond and good bond areas of a sample test specimen, showing a difference of more than 20 dB in the amplitude.

### CONCLUSION

Ultrasonic guided wave techniques are global nondestructive testing methods in nature and can provide broad possibilities of mode control and feature selection. When guided waves propagate in structures with corrosion defects, many phenomena, such as mode cutoff and conversion, group velocity changes, mode frequency shifts, and transmission and reflection amplitude ratios, *etal*, can be observed and used to detect hidden corrosion/delamination in the structures. However, for different problems, specific selection and optimization should be made to obtain the most obvious useful features. For the interface corrosion/delamination problems, effective theoretical and numerical methods should be developed to explain the experimental phenomena, while the experimental techniques used here for the artificial interface corrosion/delamination need to be verified for the practical interface corrosion/delamination situations.

### ACKNOWLEDGEMENT

The work was supported by the Naval Air Warfare Center Aircraft. The authors are also thankful to Dr. Shaw and her graduate students at the Pennsylvania State University for providing the corroded specimens used in this work.

## REFERENCES

1. J. Krautkramer and H. Krautkramer. *Ultrasonic Testing of Materials*, p.573-579. Springer-Verlag, New York (1983)
2. L. C. Lynnworth. *Ultrasonic Measurements for Process Control: Theory, Techniques, Applications*, Academic Press, Boston (1989)
3. J. Pei, M. I. Yousuf, F. L. Degertekin, B. V. Honein, and B. T. Khuri-Yakub. *Res Nondestr Eval.* **8**: 189-197 (1996)
4. W.Zhu, J.L. Rose, J.N. Barshinger, and V. Agarvala. *Res Nondestr Eval.* **10** (1998) (in press)
5. D.N. Alleyne and P. Cawley, *IEEE Trans. Ultrason., Ferroelect., Freq. Contr.* **39**, 381-397. (1992)
6. J.L. Rose, D. Jiao, S.P. Pelts, J.N. Barshinger, and M.J. Quarry, "Hidden corrosion detection with guided waves", *NACE*, New Orleans, LA, March 10<sup>th</sup>-14<sup>th</sup>, (1997).